CrystEngComm

PAPER

View Article Online
View Journal

Published on 07 December 2018. Downloaded by University of New England on 1/20/2019 11:30:28 PM.

Check for updates

Cite this: DOI: 10.1039/c8ce01658e

Controlled introduction of metal cations into polymerizable ionic liquid-polyoxomolybdate hybrid crystals†

Jun Kobayashi,[a] Toshiyuki Misawa, [a] Chihiro Umeda,[b] Toru Isono,[b] Seiji Ono,[b] Haruo Naruke,[c] Yosuke Okamura, [b] Shinichi Koguchi,[a] Masashi Higuchi,[b] Yu Nagase[b] and Takeru Ito *[a]

Received 28th September 2018,
Accepted 7th December 2018

DOI: 10.1039/c8ce01658e

rsc.li/crystengcomm

A polymerizable ionic-liquid cation having methacryl group and imidazolium moieties (denoted as $\mathrm{MAImC_1}$) was successfully hybridized with octamolybdate ($\mathrm{Mo_8O_{26}}^{4-}$, $\mathrm{Mo_8}$) to obtain inorganic–organic hybrid crystals containing monovalent metal cations. The hybrid crystals were initially prepared as sodium ion-containing hybrid crystal of $\mathrm{MAImC_1}$–Na–$\mathrm{Mo_8}$. The sodium cations in $\mathrm{MAImC_1}$–Na–$\mathrm{Mo_8}$ were exchangeable to other monovalent metal cations such as silver or potassium to form hybrid crystals of $\mathrm{MAImC_1}$–Ag–$\mathrm{Mo_8}$ or $\mathrm{MAImC_1}$–K–$\mathrm{Mo_8}$. Their molecular and crystal structures were clearly revealed by single crystal X-ray analyses. The $\mathrm{MAImC_1}$–Na–$\mathrm{Mo_8}$ hybrid crystal worked as the hybrid monomer, and was found polymerizable by a radical polymerization using AIBN as an initiator to obtain inorganic–organic polymers (P-$\mathrm{MAImC_1}$–Na–$\mathrm{Mo_8}$). The conductivities of the hybrid monomer and polymer consisting of $\mathrm{MAImC_1}$–Na–$\mathrm{Mo_8}$ were investigated.

Introduction

Rechargeable batteries such as lithium-ion or sodium-ion batteries are now being applied to power sources.[1–5] For the future usage in motor vehicles working at intermediate temperature (373 to 573 K), solid electrolytes with high conductivity are demanded to improve thermal stability and energy efficiency. Inorganic–organic hybrid materials have potential for the construction of highly conductive solid electrolytes as functionalized crystalline materials.[6–10] We can expect synergy of the merits derived from inorganic and organic components as observed in molecular conductors.[7] The introduction of metal cations into such hybrid materials can provide functions such as ionic conductivity[8,9] and ion-exchanging property.[10]

Polyoxometalate (POM) cluster anions are promising candidates as inorganic components to construct functional hybrid materials.[11–24] Hybridizing POMs with ionic-liquids[25–29] is advantageous for the emergence of conductive properties. The amphiphilic ionic-liquids and polymerizable ionic-liquid have been also utilized to build up hybrid crystals with POMs,[30–37] and some of them exhibit proton conductivities.[32–34]

The selective introduction of metal cations into the POM hybrid crystals has to be realized for the emergence of designed functions such as ionic conduction. A promising option is to use octamolybdate ($[\mathrm{Mo_8O_{26}}]^{4-}$, $\mathrm{Mo_8}$) anion. The $\mathrm{Mo_8}$ anion has several isomers represented by β-type and γ-type (Fig. 1a),[38–40] and the β-$\mathrm{Mo_8}$ anion tends to coordinate to coexisting metal cations in the solid states.[41–45] The controlled introduction of monovalent metal cations was realized also in POM-surfactant hybrid crystals by utilizing the $\mathrm{Mo_8}$ isomerization reactions.[46–48] In this introduction method of metal cations, the composition can be easily designed by simply changing the kind of coexisting metal cation under mild conditions near the room temperature. The hybrid crystals containing $\mathrm{Na^+}$ are applicable to the solid electrolytes or electrode materials for sodium-ion batteries.

Here we report another successful system of metal cation-containing inorganic–organic hybrid crystals. The hybrid crystals were constructed from polymerizable ionic-liquid (MA-$\mathrm{ImC_1}$, Fig. 1) and β- or γ-$\mathrm{Mo_8}$ anion for the first time. $\mathrm{Na^+}$, $\mathrm{Ag^+}$, and $\mathrm{K^+}$ were introduced into the $\mathrm{MAImC_1}$–$\mathrm{Mo_8}$ hybrid crystals ($\mathrm{MAImC_1}$–Na–$\mathrm{Mo_8}$ (**1**), $\mathrm{MAImC_1}$–Ag–$\mathrm{Mo_8}$ (**2**), $\mathrm{MAImC_1}$–K–$\mathrm{Mo_8}$ (**3**)) in a controlled manner by changing the coexisting monovalent cation under the mild synthetic conditions. The metal cations formed one- or two-dimensional network with the $\mathrm{Mo_8}$ anions, the dimensionality of which

---

[a] Department of Chemistry, School of Science, Tokai University, Hiratsuka 259-1292, Japan. E-mail: takeito@keyaki.cc.u-tokai.ac.jp; Fax: +81 463 58 9543; Tel: +81 463 58 1211 ex. 3737
[b] Department of Applied Chemistry, School of Engineering, Tokai University, Hiratsuka 259-1292, Japan
[c] Chemical Resources Laboratory, Tokyo Institute of Technology, Midori-ku, Yokohama 226-8503, Japan

† CCDC 1870335–1870337. For crystallographic data in CIF or other electronic format see DOI: 10.1039/c8ce01658e

Published on 07 December 2018. Downloaded by University of New England on 1/20/2019 11:30:28 PM.

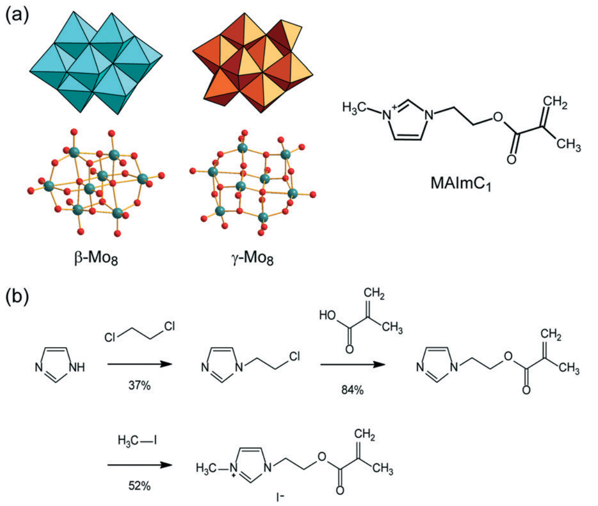

Fig. 1 Molecular structure of components. a) Octamolybdate (Mo_8) anions in ball and stick (green: Mo, red: O) and polyhedral representations (left), and polymerizable ionic-liquid ($MAImC_1$) cation (right). b) Synthetic route of $MAImC_1$-I.

depended on the size of metal cations. Na^+-containing hybrid crystal of **1** was successfully polymerized by a radical polymerization as the inorganic–organic hybrid "monomer", and the conductivities of the inorganic–organic hybrid monomer and polymer were evaluated.

Results and discussion

Synthesis and structure of $MAImC_1$–Na–Mo_8 (1) hybrid crystal

Starting polymerizable ionic-liquid of $MAImC_1$ was synthesized as iodide salt according to the procedure previously reported (Fig. 1b, see Experimental section).[34] Pale-yellow precipitate was obtained from acidified molybdate solution by adding $MAImC_1$. The IR spectrum of the precipitate (Fig. 2a) exhibited characteristic peaks of β-Mo_8 anion[38–40] in the range of 400–1000 cm^{-1} together with peaks derived from $MAImC_1$ (methylene groups in 2800–3000 cm^{-1} and methacryl group in 1200–1800 cm^{-1}). This indicates the successful formation of $MAImC_1$–Na–Mo_8 (**1**). The presence of Na^+ cation in **1** was revealed by X-ray structure analysis (see below), and confirmed by EDX spectroscopy. IR spectrum of the single crystals of **1** (Fig. 2b) obtained by recrystallization was almost the same as that of the as-prepared **1** (Fig. 2a). The powder X-ray diffraction (XRD) pattern of the as-prepared **1** (Fig. 3a) was almost the same in the peak positions as the pattern calculated from the single crystal structure of **1** (Fig. 3b). These results demonstrate that both molecular and crystal structures of **1** were retained before and after the recrystallization process.

Single crystal X-ray structure analysis clarified the molecular structure of **1** (Table 1 and Fig. 4a). The chemical formula was $[\{CH_2{=}C(CH_3)COO(CH_2)_2\}C_3H_3N_2(CH_3)]_3Na[\beta\text{-}Mo_8O_{26}]$ (denoted as $MAImC_1$–Na–Mo_8), in which three $MAImC_1$ cations (1+ charge) were associated with one β-Mo_8 anion (4− charge) and one Na^+ cation due to the charge compensation. One Na^+ cation was sandwiched by two β-Mo_8 anions to possess eight-fold coordination environment (Na–O distance: 2.53–2.67 Å) to form one-dimensional (1D) infinite chain (Fig. 4a and 5a). The 1D chain structure was similar to those observed in Na^+-containing pyridinium surfactant crystals of β-Mo_8.[46,47]

This is the first example of the hybrid crystal constructed from polymerizable ionic-liquid of $MAImC_1$ and polyoxomolybdate. The hybrid crystal of **1**, the hybrid "monomer", was successfully polymerized to form inorganic–organic hybrid polymer as described below.

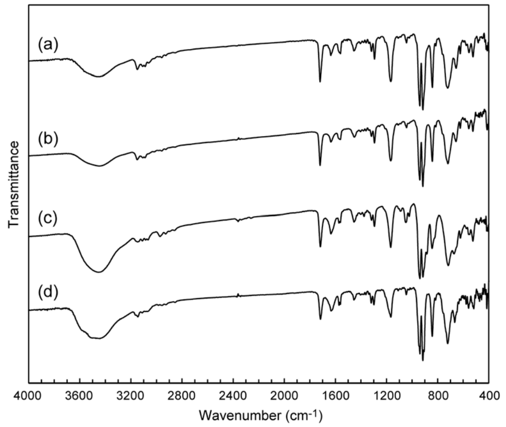

Fig. 2 IR spectra of hybrid crystals composed of $MAImC_1$ and Mo_8. a) As-prepared $MAImC_1$–Na–Mo_8 (**1**). b) Single crystal of $MAImC_1$–Na–Mo_8 (**1**). c) Single crystal of $MAImC_1$–Ag–Mo_8 (**2**). d) Single crystal of $MAImC_1$–K–Mo_8 (**3**).

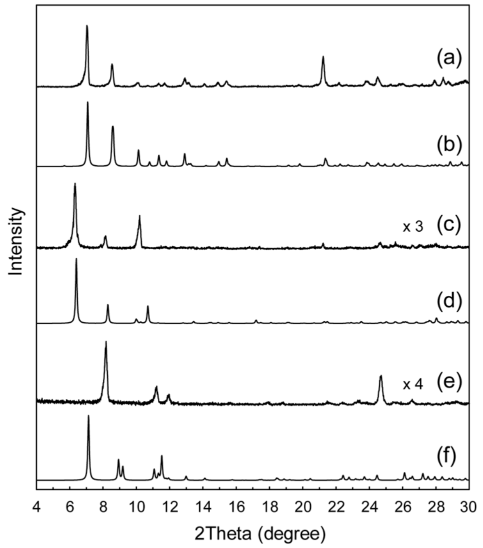

Fig. 3 Powder X-ray diffraction patterns of hybrid crystals composed of $MAImC_1$ and Mo_8. Calculated patterns were obtained from the structure by single-crystal X-ray diffraction. a) As-prepared $MAImC_1$–Na–Mo_8 (**1**). b) Calculated pattern of $MAImC_1$–Na–Mo_8 (**1**). c) Single crystal of $MAImC_1$–Ag–Mo_8 (**2**). d) Calculated pattern of $MAImC_1$–Ag–Mo_8 (**2**). e) Single crystal of $MAImC_1$–K–Mo_8 (**3**). f) Calculated pattern of $MAImC_1$–K–Mo_8 (**3**).

View Article Online

Published on 07 December 2018. Downloaded by University of New England on 1/20/2019 11:30:28 PM.

Table 1 Crystallographic data

Compound	1	2	3
Chemical formula	$C_{30}H_{45}N_6NaMo_8O_{32}$	$C_{32}H_{56}N_6Ag_2Mo_8O_{32}$	$C_{24}H_{36}N_6K_2Mo_8O_{30}$
Formula weight	1792.22	2020.07	1734.29
Crystal system	Triclinic	Triclinic	Triclinic
Space group	$P\bar{1}$	$P\bar{1}$	$P\bar{1}$
a (Å)	12.4487(7)	9.5969(7)	9.822(3)
b (Å)	14.0216(8)	10.9992(12)	10.107(4)
c (Å)	17.0849(9)	14.5293(12)	12.444(4)
α (°)	112.2762(14)	87.894(12)	85.67(3)
β (°)	93.2135(15)	72.005(9)	86.14(3)
γ (°)	105.0974(15)	75.7836(10)	78.71(3)
V (Å^3)	2624.1(3)	1412.7(2)	1206.2(7)
Z	2	1	1
ρ_{calcd} (g cm^{-3})	2.268	2.374	2.387
T (K)	193	93	93
μ(Mo Kα) (mm^{-1})	1.951	2.478	2.276
No. of reflections measured	41 831	25 493	15 617
No. of independent reflections	11 944	6479	5482
R_{int}	0.0712	0.0470	0.2095
No. of parameters	700	365	295
R_1 ($I > 2\sigma(I)$)	0.0768	0.0246	0.0622
wR_2 (all data)	0.1742	0.0577	0.1874

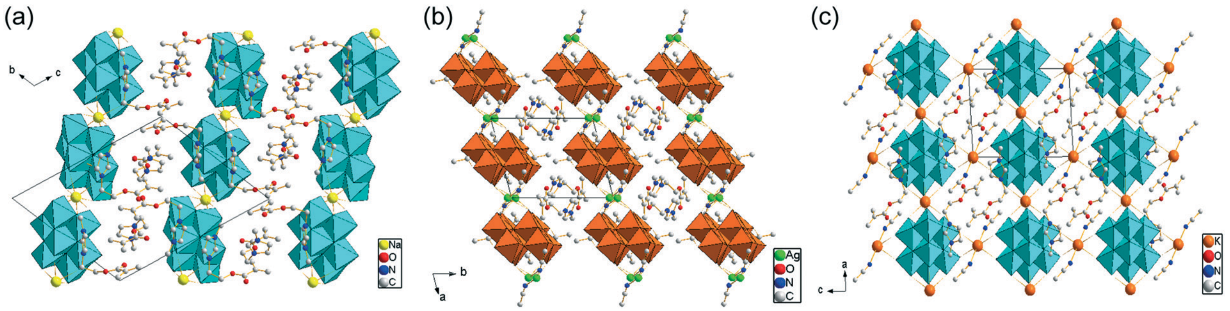

Fig. 4 Crystal structure of hybrid crystals composed of $MAImC_1$ and Mo_8 (C: gray, N: blue, O: red, Na: yellow, Ag: green, K: orange; Mo_8 anions in polyhedral representations). a) $MAImC_1$–Na–Mo_8 (**1**). b) $MAImC_1$–Ag–Mo_8 (**2**). c) $MAImC_1$–K–Mo_8 (**3**).

Synthesis and structure of $MAImC_1$–Ag–Mo_8 (2) hybrid crystal

The Na^+ cation in **1** was successfully exchanged by other monovalent metal cations. By the recrystallization process under the presence of $AgNO_3$, Ag^+-introduced hybrid crystal of $MAImC_1$–Ag–Mo_8 (**2**) was isolated as single crystals. The IR spectra (Fig. 2c) of **2** suggested the presence of β-Mo_8 anion, but the single crystal X-ray structure analysis unveiled that **2** contained γ-type Mo_8 (see below). The γ-Mo_8 was coordinated ethoxo ligands, and the Mo atoms possessed only six-fold coordination environment. Therefore, to distinguish the ethoxo-grafted γ-Mo_8 and β-Mo_8 by IR spectra was quite difficult. The powder XRD pattern of **2** (Fig. 3c) was almost the same in the peak positions as the pattern calculated from the single crystal structure of **2** (Fig. 3d), suggesting the same molecular and crystal structures at ambient temperature and 93 K. Slight differences in the peak intensity and position of the patterns may be due to the difference in the measurement temperature (powder: ambient temperature, single crystal: 93 K).

The formula of **2** was ambiguously determined to be $[\{CH_2{=}C(CH_3)COO(CH_2)_2\}C_3H_3N_2(CH_3)]_2Ag_2[\gamma\text{-}Mo_8O_{24}(OC_2H_5)_4]\cdot 2CH_3CN$ ($MAImC_1$–Ag–Mo_8, Table 1). The crystal packing is shown in Fig. 4b. The Mo_8 anion in **2** was γ-Mo_8 coordinated by four ethoxo ligands.[31] The dissolved β-Mo_8 from **1** reacted with ethanol to isomerize into ethoxo-grafted γ-Mo_8 anions, which reprecipitated as the crystals of **2**. Two $MAImC_1$ cations (1+ charge) and two Ag^+ were associated with one γ-Mo_8 anion (4− charge) to form 1D infinite chain structure (Fig. 5b). One acetonitrile molecule of crystallization was bonded to each Ag^+ cation. Each Ag^+ cation possessed six-fold coordination environment consisting of five Ag–O bonds (distance: 2.41–2.67 Å) and one Ag–N bond with a distance of 2.37 Å. The Ag–Ag bond distance was 3.08 Å. The 1D chain structure was similar to those observed in Na^+-containing ionic-liquid surfactant crystals of the ethoxo-grafted γ-Mo_8 anions.[31]

Synthesis and structure of $MAImC_1$–K–Mo_8 (3) hybrid crystal

K^+ cation was also successfully introduced into the hybrid crystals consisting of $MAImC_1$ and β-Mo_8. The recrystallization under the presence of KCl led the formation of the hybrid crystal of $MAImC_1$–K–Mo_8 (**3**). The IR spectrum (Fig. 2d) of **3**

Published on 07 December 2018. Downloaded by University of New England on 1/20/2019 11:30:28 PM.

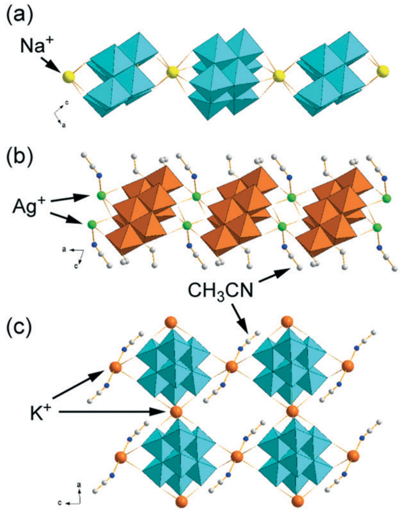

Fig. 5 Molecular arrangements of Mo_8 anions in the hybrid crystals composed of $MAImC_1$ and Mo_8 (C: gray, N: blue, O: red, Na: yellow, Ag: green, K: orange; Mo_8 anions in polyhedral representations). a) $MAImC_1$–Na–Mo_8 (**1**). b) $MAImC_1$–Ag–Mo_8 (**2**). c) $MAImC_1$–K–Mo_8 (**3**).

indicated that the β-Mo_8 anions were hybridized in **3**, being confirmed by the single crystal X-ray structure analysis. The powder XRD pattern of **3** (Fig. 3e) was different from that calculated from the single crystal structure of **3** (Fig. 3f), which suggests the change in the bulk structures owing to the removal of the solvent of crystallization (acetonitrile, see below).

The crystal of **3** had a composition of $[\{CH_2{=}C(CH_3)COO(CH_2)_2\}C_3H_3N_2(CH_3)]_2K_2[\beta\text{-}Mo_8O_{26}]\cdot 2CH_3CN$ ($MAImC_1$–K–Mo_8, Table 1, Fig. 4c). Two $MAImC_1$ cations (1+ charge) and two K^+ were associated with one β-Mo_8 anion (4− charge). In **3**, the β-Mo_8 anions and K^+ cations formed two-dimensional (2D) layered structures (Fig. 5c), being different from **1** and **2**. There were two crystallographically independent K^+ cations as shown in Fig. 5c: one K^+ cation was sandwiched by two β-Mo_8 anions to possess eight-fold coordination environment (K–O distance: 2.72–2.89 Å). The other K^+ cation was in the six-fold coordination environment by four O atoms from β-Mo_8 (K–O distance: 2.70–2.82 Å) and two crystallographically equivalent N atoms from the acetonitrile molecules of crystallization with a distance of 2.87 Å.

The changes in the arrangement of the β-Mo_8 or γ-Mo_8 anion and metal cation will be owing to the size of metal cation. The larger size of metal cations led to an increase in the dimensionality from 1D to 2D. Smaller metal cations of Na^+ (1.18 Å in ionic radius)[49] and Ag^+ (1.15 Å)[49] formed 1D chain structure, while larger K^+ cation (1.38 Å in 6-fold coordination; 1.51 Å in 8-fold coordination)[49] resulted in 2D layered structure. This connectivity between the Mo_8 anions and metal cations was relevant to other β-Mo_8 hybrids.[45,48]

Conductivity of $MAImC_1$–Na–Mo_8 (1) hybrid monomer and polymer

Conductivity of **1** was investigated by alternate current (AC) impedance spectroscopy. At first, the as-prepared hybrid "monomer" of **1** was evaluated under anhydrous atmosphere (dry N_2, 438 K). The Nyquist spectrum showed a suppressed half circle in the high- and medium-frequency regions and an inclined line in the low-frequency region (Fig. 6). The equivalent circuit employed here is shown in the inset of Fig. 6. It consists of bulk resistance and capacitance (R_b and C_b), grain boundary resistance and capacitance (R_{gb} and C_{gb}), and charge transfer resistance (R_{ct}) along with double layer capacitance (C_{dl}). Z_W represents the Warburg impedance. The red line in Fig. 6 represents simulated data with the equivalent circuit successfully reproducing the measured spectrum. The estimated value of R_b was 9.8×10^3 Ω, from which the conductivity of **1** was calculated to be 7.8×10^{-6} S cm^{-1}. The carrier in the hybrid monomer of **1** is plausibly considered to be Na^+ cation.

The inorganic–organic hybrid polymer was successfully synthesized by the radical polymerization of **1** by using 2,2′-azobis(isobutyronitrile) (AIBN) as an initiator. The resulting polymer (P-$MAImC_1$–Na–Mo_8) was obtained as colourless precipitates derived from polymerizable cation,[24,34] while several POM hybrid polymers have been prepared with POMs having covalently-grafted polymerizable group or with cationic polymers.[23,50–61] IR spectrum of hybrid polymer of P-$MAImC_1$–Na–Mo_8 (Fig. 7a) exhibited characteristic peaks of the β-Mo_8 anion in the range of 400–1000 cm^{-1}, the same as that of the hybrid monomer of **1** (Fig. 2a and b). This confirmed successful polymerization of the hybrid monomer of **1** with the molecular structures retained. Fig. 7b shows powder XRD patterns of the hybrid monomer and polymer consisting of $MAImC_1$–Na–Mo_8. XRD patterns of P-$MAImC_1$–Na–Mo_8 hybrid polymer did not show distinct peak except for halo patterns typical for amorphous polymer phase, supporting the successful polymerization of the hybrid monomer of **1**. Some weak peaks in the XRD patterns of P-$MAImC_1$–Na–Mo_8 were different from those of **1** in their positions, and may be derived from rather ordered structure of P-$MAImC_1$–Na–Mo_8. In addition, solid-state ^{13}C-magic angle spinning (MAS) NMR

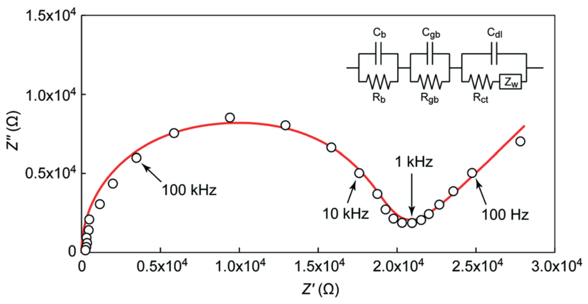

Fig. 6 Nyquist spectrum (open circles) of as-prepared hybrid monomer of $MAImC_1$–Na–Mo_8 (**1**) at 438 K under anhydrous atmosphere and simulated spectrum (red line) based on an equivalent electronic circuit in the figure. The parameters obtained by the fitting are as follows: $R_b = 9.8 \times 10^3$ Ω, $R_{gb} = 9.3 \times 10^3$ Ω, $R_{ct} = 1.5 \times 10^3$ Ω, $C_b = 2.6 \times 10^{-8}$ F, $C_{gb} = 8.2 \times 10^{-9}$ F, $C_{dl} = 1.0 \times 10^{-6}$ F, $\sigma = 1.4 \times 10^4$ Ω $s^{-1/2}$ $\left(Z_w = (1-j)\sigma/\sqrt{\omega}\right)$.

This journal is © The Royal Society of Chemistry 2018

Published on 07 December 2018. Downloaded by University of New England on 1/20/2019 11:30:28 PM.

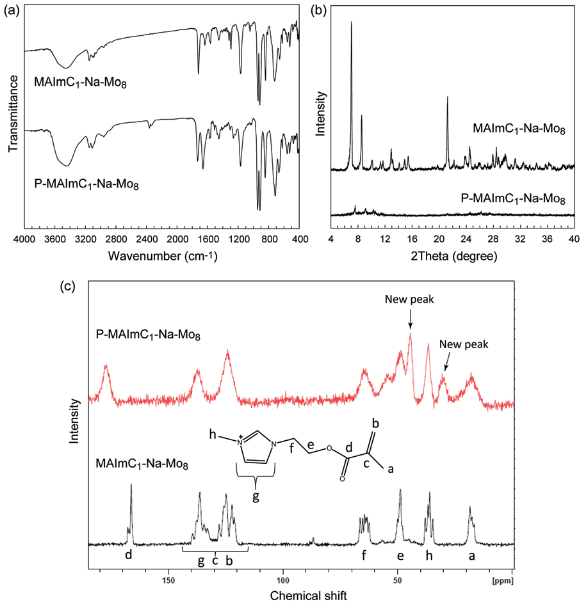

Fig. 7 a) IR spectra of hybrid monomer of MAImC$_1$–Na–Mo$_8$ (**1**) (upper) and P-MAImC$_1$–Na–Mo$_8$ hybrid polymer (bottom). b) Powder X-ray diffraction patterns of hybrid monomer of MAImC$_1$–Na–Mo$_8$ (**1**) (upper) and P-MAImC$_1$–Na–Mo$_8$ hybrid polymer (bottom). c) ^{13}C MASNMR spectra of hybrid monomer of MAImC$_1$–Na–Mo$_8$ (**1**) (bottom) and P-MAImC$_1$–Na–Mo$_8$ hybrid polymer (upper).

spectra were compared before and after the polymerization of **1**. After the polymerization (Fig. 7c, upper), two peaks at 36.4 and 44.4 ppm assigned to the methylene group newly appeared, and peaks between 118 and 140 ppm assigned to the carbon–carbon double bond (Fig. 7c, peaks b, c and g) in methacryloyl and imidazolium groups changed to the broad two peaks at 123.7 ppm and 137.4 ppm (Fig. 7c, upper), which would be carbon peaks derived from only imidazolium group. Furthermore, it was obvious that the carbonyl carbon peak of methacryloyl group (Fig. 7c, peak d) was shifted from 166.3 ppm to 177.3 ppm (Fig. 7c, upper) after the polymerization. Therefore, it was found from these ^{13}C-NMR spectra that methacryloyl groups of the monomer, **1**, completely converted to methylene structure in the polymer, P-MAImC$_1$–Na–Mo$_8$. These changes indicated the successful polymerization of the hybrid monomer of **1** by the radical coupling reaction between the methacryloyl groups in MAImC$_1$ cations of each monomer component, although the molecular weight of P-MAImC$_1$–Na–Mo$_8$ could not be measured by gel permeation chromatography (GPC) owing to the low solubility of P-MAImC$_1$–Na–Mo$_8$. The presence of Na$^+$ cations in the hybrid polymer of P-MAImC$_1$–Na–Mo$_8$ was confirmed by EDS spectroscopy.

The hybrid polymer of P-MAImC$_1$–Na–Mo$_8$ exhibited a conductivity of 5.0×10^{-10} S cm^{-1} at 363 K without additional humidity (relative humidity (RH) ~30%) (Fig. 8a). On the other hand, the conductivity of P-MAImC$_1$–Na–Mo$_8$ increased by five orders of magnitude to reach 5.1×10^{-5} S cm^{-1} at 363 K under additional humidity (RH 95%) (Fig. 8b). The carrier of the conduction is plausibly considered to be Na$^+$ cations, while the detailed feature is under investigation.

Experimental

Materials and methods

Materials. All chemical reagents except for the ionic-liquid imidazolium (MAImC$_1$) cation were purchased from Wako Pure Chemical Industries, Ltd. (Wako) and Tokyo Chemical Industry Co., Ltd. (TCI). 2,2′-Azobis(isobutyronitrile) (AIBN, Wako) was purified by recrystallization from ethanol before use, and the other reagents were employed as received. MAImC$_1$ was prepared as iodide salt (MAImC$_1$-I) according to the previously described procedures.[34]

Methods. IR spectra (as KBr pellet) were recorded on a Jasco FT/IR-4200ST spectrometer. Powder X-ray diffraction (XRD) patterns were measured with a Rigaku MiniFlex300 diffractometer by using Cu Kα radiation (λ = 1.54056 Å) at ambient temperature. CHN elemental analyses were performed with a PerkinElmer 2400II elemental analyser. Energy dispersive X-ray spectroscopy (EDS) was performed on a Hitachi Miniscope TM3030. Solution ^{1}H NMR spectroscopy was conducted with a Bruker AVANCE-500 NMR spectrometer (500 MHz) at room temperature. Solid-state ^{13}C-magic angle spinning (MAS) NMR spectra (MAS rare 8 kHz) were recorded with a Bruker AVANCE III 400WB spectrometer by using cross polarization.

Conductivity measurements were carried out by alternating current (AC) impedance method. Pelletized powder samples sandwiched with Pt electrodes were employed. Anhydrous conductivities were measured in a frequency range from 20 to 1.0×10^7 Hz using a Wayne Kerr 6510P inductance–capacitance–resistance (LCR) meter under dry nitrogen atmosphere. Conductivities under ambient atmosphere of relative humidity (RH) ~30% and fully humidified conditions of RH 95% were measured in a frequency range from 20 to 1.0×10^6 Hz using an Agilent technologies 4284A or a HIOKI 3532-50 LCR meter coupled with an Espec SH-641 bench-top type temperature and humidity chamber.

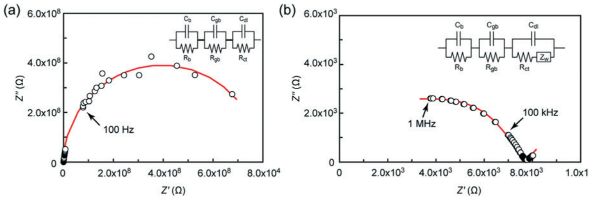

Fig. 8 Nyquist spectra (open circles) of hybrid polymer of MAImC$_1$–Na–Mo$_8$ (P-MAImC$_1$–Na–Mo$_8$) and simulated spectrum (red line) based on an equivalent electronic circuit in the figure. a) Measured at 363 K without additional humidity (RH ~30%). The parameters obtained by the fitting are as follows: $R_b = 3.8 \times 10^8\ \Omega$, $R_{gb} = 4.0 \times 10^8\ \Omega$, $R_{ct} = 7.0 \times 10^6\ \Omega$, $C_b = 1.5 \times 10^{-9}$ F, $C_{gb} = 1.5 \times 10^{-9}$ F, $C_{dl} = 2.0 \times 10^{-8}$ F. b) Measured at 363 K with additional humidity (RH 95%). The parameters obtained by the fitting are as follows: $R_b = 3.4 \times 10^3\ \Omega$, $R_{gb} = 3.5 \times 10^3\ \Omega$, $R_{ct} = 7.5 \times 10^2\ \Omega$, $C_b = 9.5 \times 10^{-8}$ F, $C_{gb} = 1.8 \times 10^{-8}$ F, $C_{dl} = 4.0 \times 10^{-6}$ F, $\sigma = 4.0 \times 10^2\ \Omega\ \mathrm{s}^{-1/2}$ $\left(Z_w = (1-j)\sigma/\sqrt{\omega}\right)$.

Published on 07 December 2018. Downloaded by University of New England on 1/20/2019 11:30:28 PM.

Synthetic procedures

$MAImC_1$-I

Synthesis of 1-(2-chloroethyl)-1H-imidazole. The solution of imidazole 2.04 g (30 mmol) in 1,2-dichloroethane (30 mL) was added to tetrabutylammonium bromide 0.20 g (0.6 mmol) and K_2CO_3 0.82 g (6 mmol). The result mixture was stirred at 358 K for 5 h. The mixture was extracted with $CHCl_3$, and the organic layer was washed with water, dried ($MgSO_4$) and evaporated. The product was isolated by silica gel column chromatography to give the title compound (1.47 g, 37%) as a colourless liquid. ^1H NMR (500 MHz, $CDCl_3$) δ 3.76 (t, J = 10 Hz, 2H), 4.28 (t, J = 10 Hz, 2H), 6.98 (s, 1H), 7.10 (s, 1H), 7.54 (s, 1H).

Synthesis of 2-(1H-imidazol-1-yl) ethyl methacrylate. The solution of 1-(2-chloroethyl)-1*H*-imidazole 1.13 g (13.2 mmol) in THF (25 mL) was added to methacrylic acid 1.47 g (11.2 mmol) and K_2CO_3 3.58 g (25.9 mmol). The resulting mixture was stirred at 339 K overnight. The mixture was extracted with $CHCl_3$, and the organic layer was washed with water, dried ($MgSO_4$), and evaporated. The product was isolated by silica gel column chromatography to give 1.70 g (84%) of the title compound as a colourless liquid. ^1H NMR (500 MHz, $CDCl_3$) δ 1.93 (s, 3H), 4.25 (t, J = 5 Hz, 3H), 4.40 (t, J = 5 Hz, 3H), 5.61 (s, 1H), 6.10 (s, 1H), 6.96 (s, 1H), 7.08 (s, 1H), 7.51 (s, 1H).

Synthesis of 1-(2-(methacryloyloxy) ethyl)-3-methyl-1H-imidazol-3-ium iodide ($MAImC_1$-I). The solution of 2-(1*H*-imidazol-1-yl) ethyl methacrylate 10 g (55.6 mmol) in 39.4 g (278 mmol) iodomethane was stirred at 333 overnight. The product was isolated by silica gel column chromatography to give 8.45 g (52%) of the title compound as a brown liquid. ^1H NMR (500 MHz, $CDCl_3$) δ 1.85 (s, 3H), 3.86 (s, 3H), 4.43 (t, J = 5.5 Hz, 3H), 4.52 (t, J = 5.5 Hz, 3H), 5.72 (s, 1H), 6.04 (s, 1H), 7.71 (s, 1H), 7.79 (s, 1H), 9.15 (s, 1H).

$MAImC_1$–Na–Mo_8 hybrid monomer (1)

As-prepared **1** was precipitated by a cation exchange reaction. $Na_2MoO_4\cdot 2H_2O$ (1.0 g, 4.13 mmol) was dissolved in 10 mL of H_2O, and the pH was adjusted to 4.0 by 6 M HCl. To the obtained clear colourless solution was added an ethanol solution (10 mL) of $MAImC_1$-I (0.52 g, 1.55 mmol) to form colourless suspension. The precipitates were isolated by filtration, and dried in the ambient atmosphere to obtain pale-yellow powder of as-prepared **1** (yield: 36%). An acetonitrile/ethanol solution (15 mL, 1 : 1 (v/v)) of as-prepared **1** (0.05 g) was heated at 348 K for 3 hours, and then the supernatant was stored at 303 K or slowly evaporated at room temperature to obtain colourless plates of **1**. Anal. calcd for $C_{30}H_{45}N_6NaMo_8O_{32}$ (%): C, 20.10; H, 2.53; N, 4.69. Found: C, 19.87; H, 2.52; N, 4.71. IR (KBr, ν/cm^{-1}): 3149w, 3115w, 2960w, 2925w, 1719w, 1637w, 1562w, 1450w, 1319w, 1296w, 1166w, 1012w, 971m, 920s, 884w, 795s, 649w, 622w, 537w. 3151w, 3090w, 3014w, 2959w, 2926w, 1719s, 1632w, 1559w, 1445w, 1403w, 1380w, 1362w, 1317w, 1294m, 1254w, 1169s, 1043w, 939s, 915s, 841m, 814w, 764w, 717s, 653m, 624w, 553w, 523w cm^{-1}.

$MAImC_1$–Ag–Mo_8 hybrid monomer (2)

An acetonitrile/ethanol solution (15 mL, 1 : 1 (v/v)) containing as-prepared **1** (0.03 g) and solid $AgNO_3$ (0.02 g) was heated at 348 K for 3 hours, and then the supernatant was kept at 303 K to obtain colourless plates of **2**. Anal. calcd for $C_{22}H_{36}N_4Ag_2Mo_8O_{31}$ (%): C, 14.39; H, 1.98; N, 3.05. Found: C, 14.74; H, 2.00; N, 3.27. IR (KBr, ν/cm^{-1}): 3147w, 3110w, 3085w, 2971w, 2928w, 1717 m, 1635w, 1572w, 1455w, 1402w, 1376w, 1317w, 1295w, 1168 m, 1092w, 1049w, 1023w, 938s, 915s, 884 m, 844m, 717s, 671m, 622w, 557w, 525w cm^{-1}.

$MAImC_1$–K–Mo_8 hybrid monomer (3)

Colourless needles of **3** were obtained by a similar procedure for **2**. Solid KCl (0.02 g) was employed instead of $AgNO_3$. Anal. calcd for $C_{20}H_{30}N_4K_2Mo_8O_{30}$ (%): C, 14.54; H, 1.83; N, 3.39. Found: C, 14.46; H, 1.96; N, 3.41. IR (KBr, ν/cm^{-1}): 3146w, 3112w, 2984w, 2954w, 2926w, 1716m, 1634w, 1561w, 1455w, 1404w, 1362w, 1320w, 1299w, 1167m, 1045w, 938s, 916s, 843m, 817w, 721s, 667m, 634w, 558w, 518w cm^{-1}.

P-$MAImC_1$–Na–Mo_8 hybrid polymer

In a 50 mL eggplant flask, 0.407 g (0.227 mmol) of $MAImC_1$–Na–Mo_8 (**1**) and 16.0 mg (0.097 mmol) of 2,2′-azobis(isobutyronitrile) (AIBN) were dissolved in 1.8 mL of DMF. After degassing the flask, it was sealed by a three-way stopcock, and the mixture was stirred at 353 K for 20 h. Then, the reaction mixture was poured into an excess amount of ethyl acetate to precipitate the polymer. The obtained polymer was washed with methanol and dried *in vacuo* to afford 0.352 g of P-$MAImC_1$–Na–Mo_8 (yield: 86.5%), which was insoluble in any solvent, such as chloroform, THF, DMSO, DMF and NMP.

Crystallography

Single crystal X-ray diffraction measurements were performed on a Rigaku R-AXIS RAPID diffractometer for **1** and a XtaLAB P200 diffractometer for **2** and **3** using graphite monochromated Mo Kα radiation (λ = 0.71075 Å). Diffraction data were collected and processed with PROCESS-AUTO[62] for **1** and CrystalClear[63] for **2** and **3**. The structures were solved by Superflip[64] for **1** and **2** or SHELXS Version 2013/1(ref. 65) for **3** and sequentially expanded using Fourier techniques. The refinement procedure was performed by the full-matrix least-squares using SHELXL Version 2014/7 (ref. 65) through CrystalStructure software package.[66] In the refinement procedure, most non-hydrogen atoms were refined anisotropically, and some non-hydrogen atoms in **3** were refined isotropically. The hydrogen atoms on C atoms were located in calculated positions.

Conclusions

Polymerizable ionic-liquid ($MAImC_1$) was utilized to construct the inorganic–organic hybrid crystals of octamolybdate (Mo_8) anions. The hybrid crystals contained metal cations such as

Published on 07 December 2018. Downloaded by University of New England on 1/20/2019 11:30:28 PM.

Na^+, Ag^+, and K^+, which were successfully introduced by the well-controlled synthetic manner. Each metal cation was connected to Mo_8 anions, while the dimensionality changed depending on the size of metal cations. In addition, the Na^+ cation-containing hybrid crystal ($MAImC_1$–Na–Mo_8) worked as the inorganic–organic hybrid "monomer". The radical polymerization of $MAImC_1$–Na–Mo_8 with AIBN led to successful formation of the inorganic–organic hybrid polymer of P-$MAImC_1$–Na–Mo_8 without any compositional change. These hybrid monomer and polymer of $MAImC_1$–Na–Mo_8 are promising as unconventional solid electrolyte or electrode material for sodium-ion batteries due to the conductive property of ionic-liquids and redox characteristics of POMs.

Conflicts of interest

There are no conflicts to declare.

Acknowledgements

Dr. Yoshiki Oda and Dr. Tsubasa Kawaguchi (Technology Joint Management Office, Tokai University) were gratefully acknowledged for the solid-state NMR measurements. This work was financially supported in part by JSPS KAKENHI Grant Number JP26410245, and Research and Study Project of Tokai University Educational System General Research Organization.

Notes and references

1 M. S. Whittingham, *Chem. Rev.*, 2004, **104**, 4271.
2 J. B. Goodenough and K.-S. Park, *J. Am. Chem. Soc.*, 2013, **135**, 1167.
3 N. Yabuuchi, K. Kubota, M. Dahbi and S. Komaba, *Chem. Rev.*, 2014, **114**, 11636.
4 D. Kundu, E. Talaie, V. Duffort and L. F. Nazar, *Angew. Chem., Int. Ed.*, 2015, **54**, 3431.
5 P. Saha, M. K. Datta, O. I. Velikokhatnyi, A. Manivannan, D. Alman and P. N. Kumta, *Prog. Mater. Sci.*, 2014, **66**, 1.
6 U. Schubert, *Chem. Soc. Rev.*, 2011, **40**, 575.
7 E. Coronado and C. J. Gómez-García, *Chem. Rev.*, 1998, **98**, 273; E. Coronado, C. Giménez-Saiz and C. J. Gómez-García, *Coord. Chem. Rev.*, 2005, **249**, 1776.
8 T. Kato, N. Mizoshita and K. Kishimoto, *Angew. Chem., Int. Ed.*, 2006, **45**, 38.
9 I. Honma and M. Yamada, *Bull. Chem. Soc. Jpn.*, 2007, **80**, 2110.
10 R. Kawahara, S. Uchida and N. Mizuno, *Chem. Mater.*, 2015, **27**, 2092.
11 Y.-F. Song, D.-L. Long, C. Ritchie and L. Cronin, *Chem. Rec.*, 2011, **11**, 158.
12 P. Yin, D. Li and T. Liu, *Chem. Soc. Rev.*, 2012, **41**, 7368.
13 M. Nyman, *Dalton Trans.*, 2011, **40**, 8049.
14 A. Proust, B. Matt, R. Villanneau, G. Guillemot, P. Gouzerh and G. Izzet, *Chem. Soc. Rev.*, 2012, **41**, 7605.
15 A. Banerjee, B. S. Bassil, G.-V. Röschenthaler and U. Kortz, *Chem. Soc. Rev.*, 2012, **41**, 7590.
16 M. Clemente-León, E. Coronado, A. Soriano-Portillo, C. Mingotaud and J. M. Dominguez-Vera, *Adv. Colloid Interface Sci.*, 2005, **116**, 193.
17 W. Qi and L. Wu, *Polym. Int.*, 2009, **58**, 1217.
18 S. Polarz, S. Landsmann and A. Klaiber, *Angew. Chem., Int. Ed.*, 2014, **53**, 946.
19 A. Nisar and X. Wang, *Dalton Trans.*, 2012, **41**, 9832.
20 S. Herrmann, C. Ritchie and C. Streb, *Dalton Trans.*, 2015, **44**, 7092.
21 M. Sadakane and E. Steckhan, *Chem. Rev.*, 1998, **98**, 219.
22 T. Yamase, *Chem. Rev.*, 1998, **98**, 307.
23 T. Hasegawa, K. Shimizu, H. Seki, H. Murakami, S. Yoshida, K. Yoza and K. Nomiya, *Inorg. Chem. Commun.*, 2007, **10**, 1140.
24 H. Li, W. Qi, W. Li, H. Sun, W. Bu and L. Wu, *Adv. Mater.*, 2005, **17**, 2688.
25 A. B. Bourlinos, K. Raman, R. Herrera, Q. Zhang, L. A. Archer and E. P. Giannelis, *J. Am. Chem. Soc.*, 2004, **126**, 15358.
26 Y. Leng, J. Wang, D. Zhu, X. Ren, H. Ge and L. Shen, *Angew. Chem., Int. Ed.*, 2009, **48**, 168.
27 E. Rafiee and S. Eavani, *Catal. Commun.*, 2012, **25**, 64.
28 X. Chen, B. Souvanhthong, H. Wang, H. Zheng, X. Wang and M. Huo, *Appl. Catal., B*, 2013, **138-139**, 161.
29 P. G. Rickert, M. R. Antonio, M. A. Firestone, K.-A. Kubatko, T. Szreder, J. F. Wishart and M. L. Dietz, *J. Phys. Chem. B*, 2007, **111**, 4685.
30 T. Ito, R. Ide, K. Kosaka, S. Hasegawa, K. Mikurube, M. Taira, H. Naruke and S. Koguchi, *Chem. Lett.*, 2013, **42**, 1400.
31 T. Ito, K. Mikurube, K. Hasegawa, T. Matsumoto, K. Kosaka, H. Naruke and S. Koguchi, *Crystals*, 2014, **4**, 42.
32 J. Kobayashi, R. Kawahara, S. Uchida, S. Koguchi and T. Ito, *Int. J. Mol. Sci.*, 2016, **17**, 994.
33 T. Misawa, S. Koguchi, K. Niwa, Y. Kinoshita, S. Uchida and T. Ito, *Inorg. Chem. Commun.*, 2018, **96**, 24.
34 T. Ito, S. Otobe, T. Oda, T. Kojima, S. Ono, M. Watanabe, Y. Kiyota, T. Misawa, S. Koguchi, M. Higuchi, M. Kawano and Y. Nagase, *Polymers*, 2017, **9**, 290.
35 Y. Jiang, S. Liu, S. Li, J. Miao, J. Zhang and L. Wu, *Chem. Commun.*, 2011, **47**, 10287.
36 H.-J. Du, L.-W. Mi, Z.-C. Yue, Y.-Y. Niu and H.-W. Hou, *Inorg. Chim. Acta*, 2014, **409**, 418.
37 K. Wang and R. Zhuang, *Inorg. Chim. Acta*, 2017, **461**, 1.
38 W. G. Klemperer and W. Shum, *J. Am. Chem. Soc.*, 1976, **98**, 8291.
39 J. J. Cruywagen, *Adv. Inorg. Chem.*, 1999, **49**, 127.
40 S. Himeno, H. Niiya and T. Ueda, *Bull. Chem. Soc. Jpn.*, 1997, **70**, 631.
41 A. Kitamura, T. Ozeki and A. Yagasaki, *Inorg. Chem.*, 1997, **36**, 4275.
42 M. McCann, K. Maddock, C. Cardin, M. Convery and V. Quillet, *Polyhedron*, 1994, **13**, 835.
43 S.-M. Chen, C.-Z. Lu, Y.-Q. Yu, Q.-Z. Zhang and X. He, *Inorg. Chem. Commun.*, 2004, **7**, 1041.
44 H. Abbas, A. L. Pickering, D.-L. Long, P. Kögerler and L. Cronin, *Chem. – Eur. J.*, 2005, **11**, 1071.
45 A. S. Pakhomova and S. V. Krivovichev, *Inorg. Chem. Commun.*, 2010, **13**, 1463.

Published on 07 December 2018. Downloaded by University of New England on 1/20/2019 11:30:28 PM.

46 T. Ito, K. Mikurube, Y. Abe, T. Koroki, M. Saito, J. Iijima, H. Naruke and T. Ozeki, *Chem. Lett.*, 2010, **39**, 1323.

47 T. Ito, K. Mikurube, K. Hasegawa, M. Kurasawa, H. Naruke and T. Ozeki, *Chem. Lett.*, 2011, **40**, 626.

48 K. Mikurube, K. Hasegawa, T. Matsumoto, J. Kobayashi, H. Naruke and T. Ito, *Inorg. Chem. Commun.*, 2016, **73**, 45.

49 R. D. Shannon, *Acta Crystallogr., Sect. A: Cryst. Phys., Diffr., Theor. Gen. Crystallogr.*, 1976, **32**, 751.

50 P. Judeinstein, *Chem. Mater.*, 1992, **4**, 4.

51 C. R. Mayer, V. Cabuil, T. Lalot and R. Thouvenot, *Angew. Chem., Int. Ed.*, 1999, **38**, 3672.

52 C. R. Mayer and R. Thouvenot, *Chem. Mater.*, 2000, **12**, 257.

53 C. R. Mayer, R. Thouvenot and T. Lalot, *Macromolecules*, 2000, **33**, 4433.

54 J. L. Horan, A. Genupur, H. Ren, B. J. Sikora, M.-C. Kuo, F. Meng, S. F. Dec, G. M. Haugen, M. A. Yandrasits, S. J. Hamrock, M. H. Frey and A. M. Herring, *ChemSusChem*, 2009, **2**, 226.

55 A. R. Moore, H. Kwen, A. M. Beatty and E. A. Maatta, *Chem. Commun.*, 2000, 1793.

56 J. Zhang, Y. Liu, Y. Li, H. Zhao and X. Wan, *Angew. Chem., Int. Ed.*, 2012, **51**, 4598.

57 U. Tong, W. Chen, C. Ritchie, X. Wang and Y.-F. Song, *Chem. – Eur. J.*, 2014, **20**, 1500.

58 Y. Han, Y. Xiao, Z. Zhang, B. Liu, P. Zheng, S. He and W. Wang, *Macromolecules*, 2009, **42**, 6543.

59 W.-K. Miao, Y.-K. Yan, X.-L. Wang, Y. Xiao, L.-J. Ren, P. Zheng, C.-H. Wang, L.-X. Ren and W. Wang, *ACS Macro Lett.*, 2014, **3**, 211.

60 W.-K. Miao, A. Yi, Y.-K. Yan, L.-J. Ren, D. Chen, C.-H. Wang and W. Wang, *Polym. Chem.*, 2015, **6**, 7418.

61 Q. Cheng, W.-K. Miao, Y.-K. Yan and W. Wang, *Acta Polym. Sin.*, 2017, 1159.

62 PROCESS-AUTO, Rigaku Corporation, Tokyo, 2002.

63 CrystalClear, Rigaku Corporation, Tokyo, 2015.

64 L. Palatinus and G. Chapuis, *J. Appl. Crystallogr.*, 2007, **40**, 786.

65 G. M. Sheldrick, *Acta Crystallogr., Sect. A: Found. Crystallogr.*, 2008, **64**, 112.

66 CrystalStructure 4.3, Rigaku Corporation, Tokyo, 2018.

This journal is © The Royal Society of Chemistry 2018